Analytical study of Cattaneo–Christov heat flux model for a boundary layer flow of Oldroyd-B fluid*

F M Abbasi[1], M Mustafa[2], S A Shehzad[3,†], M S Alhuthali[4], and T Hayat[4,5]

[1] *Department of Mathematics, Comsats Institute of Information Technology, Islamabad* 44000, *Pakistan*
[2] *School of Natural Sciences (SNS), National University of Science and Technology (NUST), Islamabad* 44000, *Pakistan*
[3] *Department of Mathematics, Comsats Institute of Information Technology, Sahiwal* 57000, *Pakistan*
[4] *NAAM Research Group, Department of Mathematics, Faculty of Science, King Abdulaziz University, Jeddah* 21589, *Saudi Arabia*
[5] *Department of Mathematics, Quaid-I-Azam University* 45320, *Islamabad* 44000, *Pakistan*

(Received 21 June 2015; revised manuscript received 15 August 2015; published online 30 November 2015)

We investigate the Cattaneo–Christov heat flux model for a two-dimensional laminar boundary layer flow of an incompressible Oldroyd-B fluid over a linearly stretching sheet. Mathematical formulation of the boundary layer problems is given. The nonlinear partial differential equations are converted into the ordinary differential equations using similarity transformations. The dimensionless velocity and temperature profiles are obtained through optimal homotopy analysis method (OHAM). The influences of the physical parameters on the velocity and the temperature are pointed out. The results show that the temperature and the thermal boundary layer thickness are smaller in the Cattaneo–Christov heat flux model than those in the Fourier's law of heat conduction.

Keywords: Oldroyd-B fluid, Cattaneo–Christov heat flux, nonlinear analysis

PACS: 47.50.–d, 02.30.Hq, 02.30.Jr **DOI:** 10.1088/1674-1056/25/1/014701

1. Introduction

The researchers at present are engaged in exploring the flows of non-Newtonian fluids at various aspects. Non-Newtonian fluids are very popular due to their importance in our daily life. Examples of such fluids include sugar solutions, apple sauce, lubricants, shampoos, cosmetic products, tomato ketchup, and many others. There is no single constitutive relation describing the characteristics of all non-Newtonian fluids. The simplest subclass of the rate-type fluid is the Maxwell fluid. It only predicts the stress relaxation effects but not the stress retardation effects. Owing to such a disadvantage, an Oldroyd-B fluid model was proposed to investigate both stress relaxation and retardation effects. This model was studied in the past by various investigators under different flow geometries and physical aspects. Some studies on flows of an Oldroyd-B fluid can be found in Refs. [1]–[7]. Besides these, Shivakumara and Sureshkumar[8] reported the effects of flow and quadratic drag on the stability of an Oldroyd-B fluid in a porous space. Khan and Zeeshan[9] addressed the electrically conducting flow of an Oldroyd-B fluid induced by sawtooth pulses. Liu *et al.*[10] analyzed the unsteady Couette flow of an Oldroyd-B fluid with fractional derivative. The authors reported the solutions through the Laplace transform method. Swamy and Sidram[11] discussed the effect of rotation on the thermal convection flow of an Oldroyd-B fluid. The influences of viscoelastic parameters in the thermal convection flow of an Oldroyd-B fluid with constant heat flux were discussed by Niu *et al.*[12] Shivakumara *et al.*[13] addressed the thermal convection instability of an Oldroyd-B fluid saturating through a porous medium. The steady stagnation point flow of an Oldroyd-B fluid with mixed convection was numerically analyzed by Sajid *et al.*[14]

The dynamics of heat transfer phenomenon is a subject of special attention due to its abundant applications in engineering and industrial processes. Examples of such applications include wire drawing, cooper materials, nuclear reactor cooling, heat conduction in tissues, refrigeration, heat pumps, energy production, cooling of electronic devices, etc. The Fourier's law of heat conduction[15] explores the characteristics of heat transfer mechanism at various aspects. The main disadvantage of this model is that it leads to a parabolic energy equation which indicates that the initial disturbance is instantly experienced by the medium under observation. To overcome this disadvantage, Cattaneo[16] presented the modified Fourier's law of heat conduction by introducing a relaxation time term. The frame-indifferent generalization of Cattaneo's law through the implementation of Oldroyds' upper convective derivative was developed by Christov.[17] Ostoja-Starzewski[18] gave the mathematical derivation of the Maxwell–Cattaneo equation by involving a material time derivative of heat flux. The stability and uniqueness of the solutions constructed by the Cattaneo–Christov heat flux model were discussed by Tibullo and Zampoli.[19] The numerical solutions of an incompressible thermal convection fluid with the

*Project supported by the Deanship of Scientific Research (DSR) King Abdulaziz University, Jeddah, Saudi Arabia (Grant No. 32-130-36-HiCi).
†Corresponding author. E-mail: ali_qau70@yahoo.com
© 2016 Chinese Physical Society and IOP Publishing Ltd

Cattaneo–Christov model were constructed by Straughan[20] and Haddad.[21] The structural stability and uniqueness of the Cattaneo–Christov heat flux equations were reported by Ciarletta and Straughan.[22] Al-Qahtani and Yilbas[23] provided the closed form solutions of Cattaneo and stress equations via the Laplace transform method. Papanicolaou *et al.*[24] investigated the influence of the thermal relaxation time in the Cattaneo–Maxwell equations subjected to vertical and horizontal temperature gradients. Very recently, Han *et al.*[25] considered the Cattaneo–Christov heat flux model for a boundary layer flow of Maxwell fluid over a stretching sheet. The authors developed the homotopic solutions. Mustafa[26] reported the numerical and homotopic solutions for a two-dimensional flow of Maxwell fluid in a rotating frame. Bissell[27] discussed an oscillatory convection flow with the Cattaneo–Christov hyperbolic heat model.

In the present analysis, we introduce the Cattaneo–Christov heat flux model for a two-dimensional boundary layer flow of an Oldroyd-B fluid over a stretching sheet. An incompressible laminar fluid is taken into account. The governing nonlinear ordinary differential equations are solved by the optimal homotopy analysis method (OHAM).[28–33] Convergent series solutions are developed. Graphical results of dimensionless velocity and temperature fields are sketched and examined.

2. Problem development

We consider a two-dimensional boundary layer flow of an incompressible Oldroyd-B fluid over a linearly stretching sheet. The laws of conservation of mass and momentum for the incompressible fluid are

$$\frac{\partial u}{\partial x}+\frac{\partial v}{\partial y}=0, \tag{1}$$

$$u\frac{\partial u}{\partial x}+v\frac{\partial u}{\partial y}+\lambda_1\left(u^2\frac{\partial^2 u}{\partial x^2}+v^2\frac{\partial^2 u}{\partial y^2}+2uv\frac{\partial^2 u}{\partial x\partial y}\right)$$
$$=\nu\left(\frac{\partial^2 u}{\partial y^2}+\lambda_2\left(u\frac{\partial^3 u}{\partial x\partial y^2}+v\frac{\partial^3 u}{\partial y^3}-\frac{\partial u}{\partial x}\frac{\partial^2 u}{\partial y^2}-\frac{\partial u}{\partial y}\frac{\partial^2 u}{\partial y^2}\right)\right), \tag{2}$$

and the boundary conditions are

$$u=u_{\rm w}(x)=cx,\ v=0\ \ \text{at}\ \ y=0;$$
$$u\to 0\ \ \text{when}\ \ y\to\infty, \tag{3}$$

where u and v are the velocity components in the x and y directions, ν is the kinematic viscosity, λ_1 and λ_2 are the relaxation time and the retardation time, respectively, ρ is the density of the fluid, and $u_{\rm w}$ is the stretching velocity.

The Cattaneo–Christov heat flux model can be written as[17,19]

$$\boldsymbol{q}+\lambda_3\left(\frac{\partial \boldsymbol{q}}{\partial t}+\boldsymbol{V}\cdot\boldsymbol{\nabla}\boldsymbol{q}-\boldsymbol{q}\cdot\boldsymbol{\nabla}\boldsymbol{V}+(\boldsymbol{\nabla}\cdot\boldsymbol{V})\boldsymbol{q}\right)=-k\boldsymbol{\nabla}T, \tag{4}$$

where $\boldsymbol{q}$ is the heat flux, λ_3 is the relaxation time of the heat flux, T is the temperature, k is the thermal conductivity, and $\boldsymbol{V}$ is the velocity vector. The above equation corresponds to Fourier's law when $\lambda_3=0$.

The energy equation for the steady incompressible boundary layer flow is

$$\rho c_p\boldsymbol{V}\cdot\boldsymbol{\nabla}T=-\nabla\cdot\boldsymbol{q}. \tag{5}$$

The temperature equation governing the steady-state laminar flow is

$$u\frac{\partial T}{\partial x}+v\frac{\partial T}{\partial y}+\lambda_3\left(u\frac{\partial u}{\partial x}\frac{\partial T}{\partial x}+v\frac{\partial v}{\partial y}\frac{\partial T}{\partial y}+u\frac{\partial v}{\partial x}\frac{\partial T}{\partial y}\right.$$
$$\left.+v\frac{\partial u}{\partial y}\frac{\partial T}{\partial x}+2uv\frac{\partial^2 T}{\partial x\partial y}+u^2\frac{\partial^2 T}{\partial x^2}+v^2\frac{\partial^2 T}{\partial y^2}\right)$$
$$=\alpha\frac{\partial^2 T}{\partial y^2}. \tag{6}$$

The associated boundary conditions for the temperature are

$$T=T_{\rm w}\ \ \text{at}\ \ y=0;\quad T\to T_\infty\ \ \text{as}\ \ y\to\infty. \tag{7}$$

In the above equations, α is the thermal diffusivity, $T_{\rm w}$ is the temperature at the wall, and T_∞ is the ambient fluid temperature.

Equations (2), (3), (6), and (7) can be reduced into the dimensionless form by introducing the following new variables:

$$u=cxf'(\eta),\quad v=-\sqrt{c\nu}f(\eta),$$
$$\eta=y\sqrt{\frac{c}{\nu}},\quad \theta(\eta)=\frac{T-T_\infty}{T_{\rm w}-T_\infty}. \tag{8}$$

The equations of momentum, energy, and concentration in dimensionless form are

$$f'''+ff''-f'^2+\beta_1(2ff'f''-f^2f''')$$
$$+\beta_2(f''^2-ff'''')=0, \tag{9}$$
$$\theta''+Prf\theta'-Pr\gamma(ff'\theta'+f^2\theta'')=0, \tag{10}$$
$$f=0,\quad f'=1,\quad \theta=1\quad\text{at}\quad \eta=0, \tag{11}$$
$$f'\to 0,\quad \theta\to 0\quad\text{as}\quad \eta\to\infty, \tag{12}$$

where $\beta_1=\lambda_1 c$ and $\beta_2=\lambda_2 c$ are the Deborah numbers with respect to the relaxation time and the retardation time, $\gamma=\lambda_3 c$ is the Deborah number with respect to the relaxation time of the heat flux, and $Pr=\nu/\alpha$ is the Prandtl number.

3. Optimal homotopy analysis solutions

We solve Eqs. (9) and (10) with the boundary conditions (11) and (12) through the optimal homotopy analysis approach. Keeping in view the so-called rule of solution expression and the boundary conditions (9) and (10), it is appropriate to select the following set of base functions:[34]

$$\{\eta^k\exp(-n\eta),\quad k\geq 0,\quad n\geq 0\}. \tag{13}$$

We can express $f(\eta)$ and $\theta(\eta)$ in the following forms:[35,36]

$$f_m(\eta) = \sum_{n=0}^{\infty}\sum_{k=0}^{\infty} a_{m,n}^k \eta^k \exp(-n\eta), \tag{14}$$

$$\theta_m(\eta) = \sum_{n=0}^{\infty}\sum_{k=0}^{\infty} b_{m,n}^k \eta^k \exp(-n\eta), \tag{15}$$

where $a_{m,n}^k$ and $b_{m,n}^k$ are the coefficients. We select the following initial guess and auxiliary linear operators:

$$f_0(\eta) = 1-\exp(-\eta), \quad \theta_0(\eta) = \exp(-\eta), \tag{16}$$

$$L(f) = f''' - f', \quad L(\theta) = \theta'' - \theta. \tag{17}$$

The above initial guess and auxiliary linear operators satisfy the following properties:

$$\begin{aligned} &L(f)(C_1 + C_2\,\mathrm{e}^{\eta} + C_3\,\mathrm{e}^{-\eta}) = 0,\\ &L(\theta)(C_4\,\mathrm{e}^{\eta} + C_5\,\mathrm{e}^{-\eta}) = 0, \end{aligned} \tag{18}$$

where C_i (i = 1–5) are arbitrary constants.

3.1. The zero order deformation problems

The zero order problems are defined as[37,38]

$$\begin{aligned} &(1-q)L(f)(\bar{f}(\eta;q) - f_0(\eta))\\ &= q\hbar_f N_f(\bar{f}(\eta;q)), \end{aligned} \tag{19}$$

$$\begin{aligned} &(1-q)L(\theta)(\bar{\theta}(\eta;q) - \theta_0(\eta))\\ &= q\hbar_\theta N_\theta(\bar{f}(\eta;q), \bar{\theta}(\eta,q)), \end{aligned} \tag{20}$$

$$\bar{f}(0;q) = 0, \quad \bar{f}'(0;q) = 1, \quad \bar{\theta}(0,q) = 1, \tag{21}$$

$$\bar{f}'(\infty;q) = 0, \quad \bar{\theta}(\infty,q) = 0, \tag{22}$$

$$\begin{aligned} &N_f[\bar{f}(\eta,q)]\\ &= \frac{\partial^3 \bar{f}(\eta,q)}{\partial\eta^3} + \left(\bar{f}(\eta,q)\frac{\partial^2\bar{f}(\eta,q)}{\partial\eta^2} - \left(\frac{\partial\bar{f}(\eta,q)}{\partial\eta}\right)^2\right)\\ &+\beta_1\left(\left(\bar{f}(\eta,q)\right)^2\frac{\partial^3\bar{f}(\eta,q)}{\partial\eta^3}\right.\\ &\left.-2\bar{f}(\eta,q)\frac{\partial\bar{f}(\eta,q)}{\partial\eta}\frac{\partial^2\bar{f}(\eta,q)}{\partial\eta^2}\right)\\ &+\beta_2\left(\bar{f}(\eta,q)\frac{\partial^4\bar{f}(\eta,q)}{\partial\eta^4} - \left(\frac{\partial^2\bar{f}(\eta,q)}{\partial\eta^2}\right)^2\right), \end{aligned} \tag{23}$$

$$\begin{aligned} &N_\theta[\bar{\theta}(\eta,q), \bar{f}(\eta,q)]\\ &= \frac{\partial^2\bar{\theta}(\eta,q)}{\partial\eta^2} + Pr\bar{f}(\eta,q)\frac{\partial\bar{\theta}(\eta,q)}{\partial\eta} - Pr\gamma\left(\bar{f}(\eta,q)\frac{\partial\bar{f}(\eta,q)}{\partial\eta}\right.\\ &\left.\times\frac{\partial\bar{\theta}(\eta,q)}{\partial\eta} + \left(\bar{f}(\eta,q)\right)^2\frac{\partial^2\bar{\theta}(\eta,q)}{\partial\eta^2}\right), \end{aligned} \tag{24}$$

where $\hbar_f$ and $\hbar_\theta$ are the non-zero auxiliary parameters, $q \in [0,1]$ is the embedding parameter, and N_f and N_θ are the nonlinear operators. Let $q = 0$ and $q = 1$, then we have

$$\begin{aligned} &\bar{f}(\eta;0) = f_0(\eta), \quad \bar{\theta}(\eta,0) = \theta_0(\eta),\\ &\bar{f}(\eta;1) = f(\eta), \quad \bar{\theta}(\eta,1) = \theta(\eta). \end{aligned} \tag{25}$$

When we increase q from 0 to 1, then $f(\eta,q)$ and $\theta(\eta,q)$ vary from $f_0(\eta)$ and $\theta_0(\eta)$ to $f(\eta)$ and $\theta(\eta)$, respectively. By using the Taylor series expansion, we have

$$f(\eta,q) = f_0(\eta) + \sum_{m=1}^{\infty} f_m(\eta)q^m, \tag{26}$$

$$\theta(\eta,q) = \theta_0(\eta) + \sum_{m=1}^{\infty} \theta_m(\eta)q^m, \tag{27}$$

$$\begin{aligned} f_m(\eta) &= \frac{1}{m!}\left.\frac{\partial^m f(\eta;q)}{\partial\eta^m}\right|_{q=0},\\ \theta_m(\eta) &= \frac{1}{m!}\left.\frac{\partial^m \theta(\eta;q)}{\partial\eta^m}\right|_{q=0}. \end{aligned} \tag{28}$$

The convergence of the above series highly depends on the suitable values of $\hbar_f$ and $\hbar_\theta$. Select $\hbar_f$ and $\hbar_\theta$ properly such that equations (26) and (27) converge at $q = 1$, then we will have

$$f(\eta) = f_0(\eta) + \sum_{m=1}^{\infty} f_m(\eta), \tag{29}$$

$$\theta(\eta) = \theta_0(\eta) + \sum_{m=1}^{\infty} \theta_m(\eta). \tag{30}$$

3.2. The m-th order deformation problems

The m-th order problems can be constructed as follows:

$$L_f[f_m(\eta) - \chi_m f_{m-1}(\eta)] = \hbar_f R_f^m(\eta), \tag{31}$$

$$L_\theta[\theta_m(\eta) - \chi_m \theta_{m-1}(\eta)] = \hbar_\theta R_\theta^m(\eta), \tag{32}$$

$$f_m(0) = f_m'(0) = f_m'(\infty) = 0, \quad \theta_m(0) = \theta_m(\infty) = 0, \tag{33}$$

$$\begin{aligned} R_f^m(\eta) &= f_{m-1}'''(\eta) + \sum_{k=0}^{m-1}\left[f_{m-1-k}f_k'' - f_{m-1-k}'f_k'''\right]\\ &+\beta_1\sum_{k=0}^{m-1} f_{m-1-k}\sum_{l=0}^{k}(2f_{k-l}'f_l'' - f_{k-l}f_l''')\\ &+\beta_2\sum_{k=0}^{m-1}(f_{m-1-k}f_k'''' - f_{m-1-k}''f_k''), \end{aligned} \tag{34}$$

$$\begin{aligned} R_\theta^m(\eta) &= \theta_{m-1}'' + Pr\sum_{k=0}^{m-1}\theta_{m-1-k}f_k' - Pr\gamma\\ &\times\sum_{k=0}^{m-1} f_{m-1-k}\sum_{l=0}^{k}(f_{m-1-k}'\theta_k' + f_{m-1-k}\theta_k'). \end{aligned} \tag{35}$$

The general solutions can be written as

$$f_m(\eta) = f_m^*(\eta) + C_1 + C_2\,\mathrm{e}^{\eta} + C_3\,\mathrm{e}^{-\eta}, \tag{36}$$

$$\theta_m(\eta) = \theta_m^*(\eta) + C_4\,\mathrm{e}^{\eta} + C_5\,\mathrm{e}^{-\eta}, \tag{37}$$

where f_m^* and θ_m^* are the special solutions. The constants C_1–C_5 are given by

$$\begin{aligned} &C_3 = \left.\left(\frac{\partial f_m^*(\eta)}{\partial\eta}\right)\right|_{\eta=0}, \quad C_1 = -C_3 - f_m^*(0),\\ &C_5 = -\theta_m^*(0), \quad C_2 = C_4 = 0. \end{aligned} \tag{38}$$

The squared residuals of the governing equations are defined in the following forms:

$$E_{f,M} = \int_0^{\infty} \left[N_f \left(\sum_{j=0}^{M} f_j(\eta) \right) \right]^2 \mathrm{d}\eta, \tag{39}$$

$$E_{\theta,M} = \int_0^{\infty} \left[N_\theta \left(\sum_{j=0}^{M} f_j(\eta), \sum_{j=0}^{M} \theta_j(\eta) \right) \right]^2 \mathrm{d}\eta. \tag{40}$$

Such a kind of error is considered in various recent papers.[29–33] The best possible values of $\hbar$ at a given order of approximation may be computed by minimizing the squared residuals $E_{f,M}$ and $E_{\theta,M}$. This can be achieved through the command Minimize of the software Mathematica (see Ref. [28] for details). The optimal values of $\hbar$ for the functions f and θ are given in Tables 1 and 2.

Table 1. Optimal auxiliary parameter $\hbar$ for function f at the 15th order approximation for different β_1 when $\beta_2 = 0.5$.

β_1	Optimal $\hbar$	Minimum $E_{f,M}$
0	–0.768	4.32×10^{-22}
0.25	–0.504	1.54×10^{-11}
0.50	–0.565	2.38×10^{-11}
0.75	–0.583	3.86×10^{-11}
1.00	–0.560	4.27×10^{-10}

Table 2. Optimal auxiliary parameter $\hbar$ for function θ at 15th order approximation for different γ when $\beta_2 = 0.5$.

γ	Optimal $\hbar$	Minimum $E_{\theta,M}$
0	–0.903	8.86×10^{-12}
0.25	–0.926	1.84×10^{-9}
0.50	–0.987	8.62×10^{-8}
0.75	–0.978	1.38×10^{-6}
1.00	–0.511	2×10^{-4}

4. Analysis and discussion

Figures 1 and 2 are drawn to examine the influences of Deborah numbers β_1 and β_2 on the dimensionless velocity field $f'(\eta)$. From Fig. 1, we find that the velocity field and the momentum boundary layer thickness are decreasing functions of Deborah number β_1. The Deborah number β_1 appears due to the relaxation time. The larger Deborah number β_1 corresponds to longer relaxation time and such longer relaxation time resists the fluid flow due to lower velocity and thinner momentum boundary layer. On the other hand, an increase in the Deborah number β_2 gives an enhancement to the velocity field and the momentum boundary layer thickness (see Fig. 2). In fact, the Deborah number β_2 is directly related to the retardation time and the retardation time has an ability to enhance the fluid velocity. Here the Maxwell fluid flow case is obtained by setting $\beta_2 = 0$. Moreover, the viscous fluid case is obtained when $\beta_1 = 0 = \beta_2$.

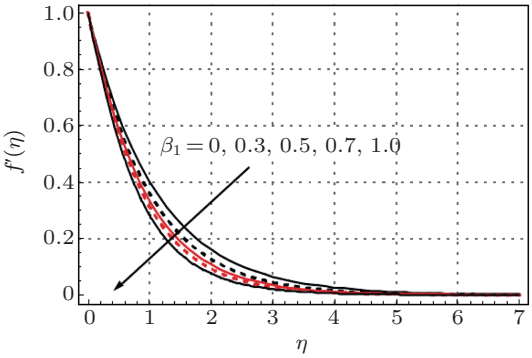


Fig. 1. (color online) Variation of dimensionless velocity field $f'(\eta)$ with η for different β_1 when $\beta_2 = 0.2$.

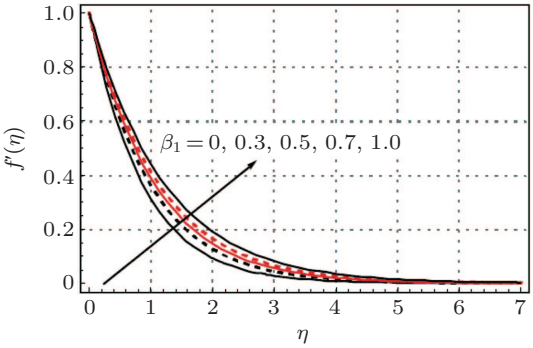


Fig. 2. (color online) Variation of dimensionless velocity field $f'(\eta)$ with η for different β_2 when $\beta_1 = 0.4$.

The variations in dimensionless temperature profile $\theta(\eta)$ corresponding to different Deborah numbers β_1 and β_2, Deborah number γ with respect to the heat flux relaxation time and Prandtl number Pr are shown in Figs. 3–6. From Figs. 3 and 4, we note that the Deborah numbers β_1 and β_2 have quite reverse effects on the temperature profile and the thermal boundary layer thickness. The temperature profile is enhanced with the increase of the Deborah number β_1, but it reduces for larger Deborah number β_2. Physically, the Deborah numbers β_1 and β_2 appear due to the relaxation time and the retardation time, respectively, and these parameters have quite opposite effects on the temperature and the heat transfer rate. The involvements with the relaxation time and the retardation time here are responsible for the reduction and enhancement of the temperature profile and the thermal boundary layer thickness. Figure 5 shows that the temperature profile and the thermal boundary layer thickness are lower for larger Deborah number γ. The Deborah number γ arises due to the heat flux relaxation time. The fluid with longer heat flux relaxation time has lower temperature, and the fluid with shorter heat flux relaxation time corresponds to higher temperature. Here the longer heat flux relaxation time is obtained when we increase the Deborah number γ. Such longer heat flux relaxation time corresponds to higher heat transfer rate and smaller temperature due to the reduction in temperature and thermal boundary layer thickness. The Cattaneo–Christov heat flux model is reduced to simple

Fourier's law of heat conduction when $\gamma = 0$. The effects of the Prandtl number on the temperature profile are explored in Fig. 6. It is observed that an increase in the Prandtl number leads to a reduction in the temperature and thermal boundary layer thickness. The Prandtl number is the ratio of momentum to thermal diffusivity. The thermal diffusivity is weaker for larger Prandtl number due to the fact that the rate of diffusion decreases. Such a reduction in the diffusion rate acts as an agent showing a reduction in the temperature and thermal boundary layer thickness. The suitable Prandtl numbers are quite essential in the industrial processes, because they are used to control the heat transfer rate during the final product.

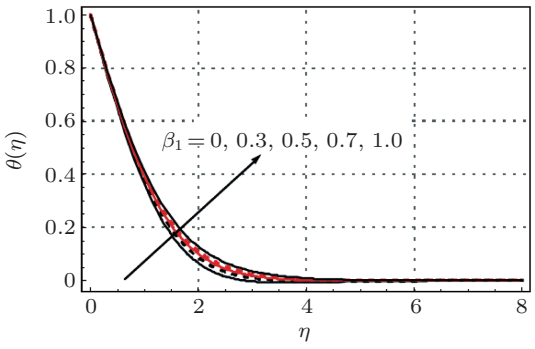


Fig. 3. (color online) Variation of dimensionless temperature field $\theta(\eta)$ with η for different β_1 when $\beta_2 = 0.2$, $\gamma = 0.3$, and $Pr = 1.4$.

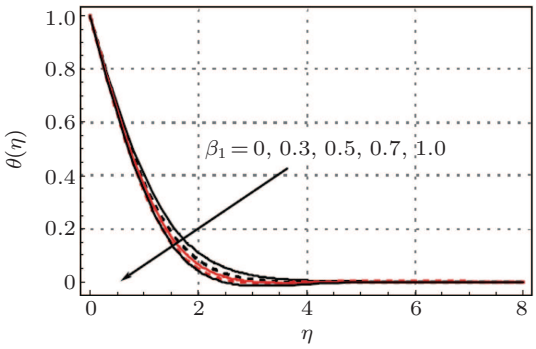


Fig. 4. (color online) Variation of dimensionless temperature field $\theta(\eta)$ with η for different β_2 when $\beta_1 = 0.4$, $\gamma = 0.3$, and $Pr = 1.4$.

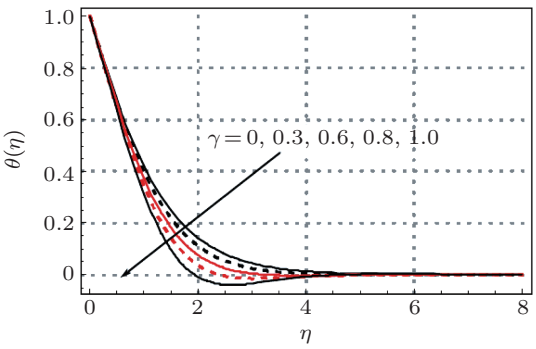


Fig. 5. (color online) Variation of dimensionless temperature field $\theta(\eta)$ with η for different γ when $\beta_1 = 0.4$, $\beta_2 = 0.2$, and $Pr = 1$.

Tables 1 and 2 present the optimal values of convergence control parameters at the 15th order of deformations for various values of β_1 and γ. Table 3 is for comparison with the numerical solutions obtained by Abel *et al.*[39] and Megahed[40] in the limiting case for different Deborah numbers β_1. From this table, we notice that our series solutions are in excellent agreement with the numerical solutions provided by Abel *et al.*[39] and Megahed.[40] Table 4 shows the comparative values of $f''(0)$ for various values of β_1 given by Sadghey *et al.*[41] and Mukhopadhyay.[42] This table also clearly indicates that our present analytical solutions are in very good agreement with the solutions of Sadghey *et al.*[41] and Mukhopadhyay[42] in the limiting case. It is also observed that the values of $f''(0)$ are larger for higher values of β_1. The Deborah number β_1 is directly proportional to the relaxation time λ_1. The λ_1 is increased for larger β_1. Such longer relaxation time reduces the fluid velocity but enhances $f''(0)$. Table 5 shows the numerical values of $f''(0)$ for different Deborah numbers β_2 when $\beta_1 = 0.4$. This table clearly presents that $f''(0)$ is reduced as Deborah number β_2 increases. The retardation time λ_2 is involved in β_2 which is enhanced for larger β_2. Such an enhancement in retardation leads to a reduction in $f''(0)$. Table 6 is for examining the temperature gradient $\theta'(0)$ for different β_2, Pr, and γ when $\beta_1 = 0.5$. Here we can see that an increase in β_2 gives rise to larger temperature gradient $\theta'(0)$. The temperature gradient $\theta'(0)$ increases for larger Pr but decreases for larger γ. The Prandtl number strongly depends on the thermal diffusivity of fluid, and the larger Prandtl number corresponds to weaker thermal diffusivity due to the fact that the temperature gradient is increased.

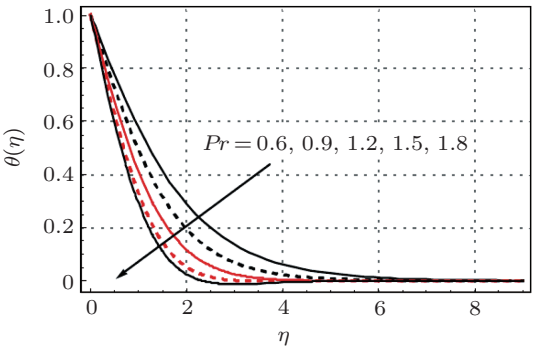


Fig. 6. (color online) Variation of dimensionless temperature field $\theta(\eta)$ with η for different Pr when $\beta_1 = 0.4$, $\beta_2 = 0.2$, and $\gamma = 0.3$.

Table 3. Comparison with $f''(0)$ obtained by Abel *et al.*[39] and Megahed[40] for different β_1 when $\beta_2 = 0$.

β_1	Abel *et al.*	Megahed	Present results
0.0	0.999962	0.999978	1.00000
0.2	1.051948	1.051945	1.05189
0.4	1.101850	1.101848	1.10190
0.6	1.150163	1.150160	1.15014
0.8	1.196692	1.196690	1.19671
1.2	1.285257	1.285253	1.28536
1.6	1.368641	1.368641	1.36873
2.0	1.447617	1.447616	1.44781

Table 4. Comparison with $f''(0)$ obtained by Sadghey *et al.*[41] and Mukhopadhyay[42] in the limiting case for different β_1 by fixing $\beta_2 = 0$.

β	Sadghey *et al.*	Mukhopadhyay	Present solutions
0.0	1.0000	0.9999963	1.00000
0.2	1.0549	1.051949	1.05189
0.4	1.10084	1.101851	1.10190
0.6	1.0015016	1.150162	1.15014
0.8	1.19872	1.196693	1.19671

Table 5. Values of $f''(0)$ for different β_2 when $\beta_1 = 0.4$.

β_2	$-f''(0)$
0.0	1.10190
0.2	1.00498
0.4	0.92986
0.6	0.86942
0.8	0.81943
1.0	0.77718

Table 6. Values of $-\theta'(0)$ for different β_2, Pr, and γ when $\beta_1 = 0.5$.

β_2	Pr	γ	$-\theta'(0)$
0.0	1.0	0.3	0.56621
0.2	1.0	0.3	0.58970
0.5	1.0	0.3	0.61671
0.3	0.8	0.3	0.51088
0.3	1.2	0.3	0.68070
0.3	1.6	0.3	0.82621
0.3	1.0	0.0	0.57276
0.3	1.0	0.2	0.59032
0.3	1.0	0.5	0.61927

5. Conclusion

We explore the properties of the Cattaneo–Christov heat flux model for a two-dimensional hydrodynamic boundary layer flow of an Oldroyd-B fluid over a stretching sheet. The obtained key features are listed below.

• The velocity field decreases while the temperature profile increases as the Deborah number β_1 increases.

• The Deborah number β_2 has quite opposite effects on the dimensionless velocity field and the temperature profile.

• The low temperature profile and thin thermal boundary layer thickness are observed in the case of the Cattaneo–Christov heat flux model in comparison to the simple Fourier's law of heat conduction.

• The larger Prandtl number leads to a reduction in the temperature profile and thermal boundary layer thickness.

References

[1] Sajid M, Abbas Z, Ali N and Javed T 2010 , *Canad. J. Phys.* **88** 635
[2] Jamil M, Fetecau C and Imran M 2011 *Commun. Nonlinear Sci. Numer. Simulat.* **16** 1378
[3] Zheng L, Liu Y and Zhang X 2012 *Nonlinear Analysis: Real World Appl.* **13** 513
[4] Li C, Zheng L, Zhang Y, Ma L and Zhang X 2012 *Commun. Nonlinear Sci. Numer. Simulat.* **17** 5026
[5] Kamran M, Imran M and Athar M 2013 *Meccanica* **48** 1215
[6] Abbasbandy S, Hayat T, Alsaedi A and Rashidi M M 2014 *Int. J. Numer. Methods Heat Fluid Flow* **24** 390
[7] Hayat T, Hussain T, Shehzad S A and Alsaedi A 2015 *Appl. Math. Mech. Eng. Edit.* **36** 69
[8] Shivakumara I S and Sureshkumar S 2008 *J. Geophys. Eng.* **5** 268
[9] Khan M and Zeeshan 2011 *Chin. Phys. Lett.* **28** 084701
[10] Liu Y, Zheng L and Zhang X 2011 *Comput. Math. Appl.* **61** 443
[11] Swamy M S and Sidram W 2013 *Fluid Dyn. Res.* **45** 015504
[12] Niu J, Shi Z H and Tan W C 2013 *J. Hydrodynamics Ser. B* **25** 639
[13] Shivakumara I S, Dhananjaya M and Ng C 2015 *Int. J. Heat Mass Transfer* **84** 167
[14] Sajid M, Ahmed B and Abbas Z 2015 *J. Egypt. Math. Soc.* **23** 440
[15] Fourier J B J 1822 *Théorie Analytique ee la Chaleur*, Paris
[16] Cattaneo C 1948 *Atti Semin. Mat. Fis. Univ. Modena Reggio Emilia* **3** 83
[17] Christov C I 2009 *Mech. Res. Commun.* **36** 481
[18] Ostoja-Starzewski M 2009 *Int. J. Eng. Sci.* **47** 807
[19] Tibullo V and Zampoli V 2011 *Mech. Res. Commun.* **38** 77
[20] Straughan B 2010 *Int. J. Heat Mass Transfer* **53** 95
[21] Haddad S A M 2014 *Int. J. Heat Mass Transfer* **68** 659
[22] Ciarletta M and Straughan B 2010 *Mech. Res. Commun.* **37** 445
[23] Al-Qahtani H and Yilbas B S 2010 *Phys. B* **405** 3869
[24] Papanicolaou N C, Christov C I and Jordan P M 2011 *Europ. J. Mec. B Fluids* **30** 68
[25] Han S, Zheng L, Li C and Zhang X 2014 *Appl. Math. Lett.* **38** 87
[26] Mustafa M 2015 *AIP Adv.* **5** 047109
[27] Bissell J J 2015 *Proceedings A*
[28] Liao S J 2010 *Commun. Nonlinear Sci. Numer. Simulat.* **15** 2003
[29] Mustafa M, Farooq M A, Hayat T and Alsaedi A 2013 *Plos One* **8** 61859
[30] Abbasbandy S and Jalili M 2013 *Numer. Algor.* **64** 593
[31] Rashidi M M, Freidoonimehr N, Hosseini A, Bég O A and Hung T K 2014 *Meccanica* **49** 469
[32] Mustafa M, Khan J A, Hayat T and Alsaedi A 2015 *IEEE Trans. Nanotech.* **14** 159
[33] Mustafa M, Khan J A, Hayat T and Alsaedi A 2015 *Int. J. Non-linear Mech.* **71** 22
[34] Zheng L, Wang L and Zhang X 2011 *Commun. Nonlinear Sci. Numer. Simulat.* **16** 731
[35] Zheng L, Niu J, Zhang X and Gao Y 2012 *Math. Comput. Modelling* **56** 133
[36] Yu R S, Cong B L, Guang H W and Zhi G Z 2012 *Chin. Phys. B* **21** 120307
[37] Hayat T, Asad S, Mustafa M and Alsulami H H 2014 *Chin. Phys. B* **23** 084701
[38] Hayat T, Asad S and Alsaedi A 2015 *Chin. Phys. B* **24** 044702
[39] Abel M S, Tawade J and Nandeppanavar M M 2012 *Meccanica* **47** 385
[40] Megahed M A 2013 *Chin. Phys. B* **22** 094701
[41] Sadeghy K, Hajibeygi H and Taghavi S M 2006 *Int. J. Non-linear Mech.* **41** 1242
[42] Mukhopadhyay S 2012 *Chin. Phys. Lett.* **29** 054703